UDK 67.017:621.793.7:544.653.23
Original scientific article/Izvirni znanstveni članek

ISSN 1580-2949
MTAEC9, 51(3)403(2017)

THE EFFECT OF CURRENT TYPES ON THE MICROSTRUCTURE AND CORROSION PROPERTIES OF Ni/NANOAl_2O_3 COMPOSITE COATINGS

VPLIV VRSTE TOKA NA MIKROSTRUKTURO IN LASTNOSTI KOROZIJE PREVLEK NA Ni/NANOAl_2O_3 KOMPOZITIH

Beata Kucharska, Agnieszka Krawczynska, Krzysztof Rożniatowski, Joanna Zdunek, Karol Poplawski, Jerzy Robert Sobiecki

Warsaw University of Technology, Woloska 141, 01-407 Warszawa, Poland
b.kucharska@inmat.pw.edu.pl

Prejem rokopisa – received: 2015-12-16; sprejem za objavo – accepted for publication: 2016-09-02

doi:10.17222/mit.2015.347

Nickel matrix composite coatings with a ceramic disperse phase have been widely investigated due to their enhanced properties, such as higher hardness and wear resistance in comparison to pure nickel. This paper describes the research on nickel and nickel-alumina coatings. The coatings were obtained from a Watts bath with the presence of nickel grain-growth inhibitors by DC (direct current), PC (pulse current) and PRC (pulsed reverse current) plating. The study includes the composite coatings of microcrystalline and nanocrystalline Ni matrix and nanometric Al_2O_3 particles. In order to ensure uniform co-embedding of the disperse phase particles with a nickel matrix and producing a stable suspension, mechanical agitation was also used. It was proved in our previous investigations that mechanical agitation is the best way of embedding nano-alumina particles in a nickel matrix. The effect of the electroplating techniques on the microstructure (SEM – scanning electron microscopy, STEM – scanning transmission electron microscopy, XRD – X-ray diffraction, surface profile) of Ni and Ni/Al_2O_3 composite coatings was investigated. In order to evaluate the corrosion resistance of the produced coatings, the corrosion studies were carried out by electrochemical impedance spectroscopy and the potentiodynamic method in a 0.5-M NaCl solution. Bode diagrams obtained by impedance spectroscopy method were established. The equivalent electric circuit and its parameters were determined to interpret impedance spectra. The corrosion current and corrosion potential were determined. Investigations of the corrosion damage to the produced surface layers were performed by scanning microscope techniques. The completed studies have shown that the type of current significantly affects the structure of the nickel and composite coatings, as well as their corrosion properties.

Keywords: nanocomposites, Ni/Al_2O_3 coatings, corrosion resistance, pulse electrodeposition

Matrike nikljevih kompozitnih oblog, razpršenih s keramično fazo, so pogosto raziskovali zaradi njihovih izboljšanih lastnosti, kot na primer zaradi večje trdote in odpornosti proti obrabi, v primerjavi s čistim nikljem. Članek opisuje raziskave na nikljevih in nikelj-aluminijevih premazih. Prevleke so bili narejene iz Watts kopeli s prisotnostjo inhibitorjev rasti zrn niklja s površinsko obdelavo z enosmernim (DC), impulznim (PC) in impulzno-povratnim (PRC) tokom. Študija vključuje mikrokristalne in nanokristalne prevleke kompozitov Ni matrike in nanometrskih Al_2O_3 delcev. Da bi zagotovili enotno delovanje vgrajevanja disperzne faze delcev z matriko Ni in pripravo stabilne suspenzije, je bilo uporabljeno tudi mehansko spodbujanje z mešanjem. Dokazano je bilo, da je mehanska spodbuda najboljši način utrjevanja delcev aluminijevega oksida v Ni matriki. Raziskan je bil učinek tehnik površinske obdelave na mikrostrukturo (SEM – elektronska mikroskopija, STEM – transmisijska elektronska mikroskopija, XRD – rentgenska difrakcija, površinski profil) niklja in Ni/Al_2O_3 kompozita. Da bi ocenili odpornost proti koroziji pri proizvedenih premazih, so bile izvedene študije korozije, ki smo jih izvedli z elektrokemijsko impedančno spektroskopijo in potenciodinamskim postopkom v 0,5 M NaCl raztopini. Vzpostavljeni Bodovi diagrami so bili dobljeni z metodo impedančne spektroskopije. Enakomerni električni krog in njegovi parametri so bili določeni za razlago impedančne spektroskopije. Določena sta bila tok korozije in korozijski potencial. Preiskave korozijskih poškodb proizvedenih površinskih slojev so bile izvedene s tehnikami mikroskopskega skeniranja. Končne preiskave so pokazale, da tip toka pomembno vpliva na strukturi nikljevih in kompozitnih prevlek, tako kot na korozijske lastnosti.

Ključne besede: nanokompoziti, Ni/Al_2O_3 premazi, odpornost proti koroziji, elektrodepozicija

1 INTRODUCTION

The introduction of new materials for transport and industry is mainly aimed at improving the performance characteristics of machine parts and equipment, often working in aggressive environments. Nanocomposite engineering metal coatings are an inspiring material group introduced in the past few years. There are various techniques of producing metallic nanocomposite materials. Electrodeposition is a simple, inexpensive and versatile one, being widely used in industry.[1–4] The structure and properties of composite surface coatings can be designed through a careful selection of the matrix and dispersed phase. Among the wide variety of coatings used for tribological applications, nickel composite coatings with alumina particles appear to have a very promising potential. The size and the amount of the inserted reinforced alumina phase determines the properties of Ni/Al_2O_3 composite coatings.[4,6] Until now, most of the works were carried out using Al_2O_3 microparticles.[2,4,7–10] However, the recent emergence of nanotechnologies has led to scientific and technological interest in the electrodeposition of Ni/Al_2O_3 nanocom-

posite coatings with Al_2O_3 particles smaller than 100 nm, mainly devoted to an increase in the abrasion resistance of material surfaces.[3,5–6,11–12]

These performance characteristics are affected primarily by the process parameters, including the electrolyte composition (e.g., the use of organic growth inhibitors), as well as the type (DC, PC, PRC), amplitude and frequency of the used current. Proper optimization of electrodeposition process of $Ni/_{nm}Al_2O_3$ coatings is faced with the fundamental problem of the agglomeration of particles in the electrolyte, and therefore an insufficient and uneven distribution of nanoparticles in the nickel matrix.[5,6] In the study the effect of the addition of a growth inhibitor and nano-alumina powder disperse phase, as well as the type of current (DC, PC, PRC) on the corrosion properties of nickel and composite Ni/Al_2O_3 coatings were examined.

Hard and wear-resistant Ni/Al_2O_3 coatings should also have good anti-corrosion properties in the environment in which they are operated.[2] The researchers' reports include mainly corrosion rate determination.[3,4,11–15] This allows a good comparison of materials in terms of corrosion resistance, but does not give information about the causes of the corrosion changes and the mechanism of corrosion. Electrochemical impedance spectroscopy can provide significant information regarding the corrosion mechanisms and susceptibility of materials to corrosion in the exposed environment. In the present work the nickel and composite coatings were examined both by the potentiodynamic method (setting the corrosion current, corrosion potential, polarization resistance) as well as electrochemical impedance spectroscopy.

2 EXPERIMENTAL PART

Nickel matrix composite coatings with a dispersed nanometric alumina phase (Aldrich Chemistry) were produced by electrochemical reduction on a copper substrate (75×15×1) mm in a Watts bath modified (or not) with benzoic sulfimide (saccharin) (**Table 1**). For comparison the nickel coatings were also produced with the same process parameters. The electrodeposition process consists of several steps, including preliminary and regular surface preparation (grinding, degreasing, digestion and finally electroplating). The processes were carried out at 45 °C at pH 4.2±0.1 using direct, pulsed and pulse reversed current. The diagram and parameters are shown in **Figure 1**. All the coatings have a thickness of approximately 30 μm, with the exception of the coatings to be examined by STEM technique (150–200 μm), for which the preparation has differed from the conventional procedure (additional application of electrospark cutting, grinding to a thickness of 4 μm and electrochemical polishing). The thickness was estimated using SEM techniques and the study was conducted on metallographic cross-sections. In order to provide the transport of alumina particles into cathode proximate areas, the bath was mechanically stirred at 400 min^{-1}.

Table 1: Bath composition
Tabela 1: Sestava kopeli

Component	Concentration (mol L^{-1})
$NiSO_4 \cdot 6\ H_2O$	1,14
$NiCl_2 \cdot 6\ H_2O$	0,17
H_3BO_3	0,57
Saccharin	0,014
Al_2O_3	0,098

A structure analysis of the alumina powder, the nickel and the nickel-alumina composite coatings was carried out using a Hitachi SU-70 (SEM) and Hitachi HD-2700 (STEM), respectively, scanning and scanning-transmission electron microscopes (both equipped with EDS – energy-dispersive X-ray spectroscopy device).

The phase composition, crystalline size, and residual stresses of the deposits were studied by the XRD technique using Cu-K_α (Philips PW-1830). The surface roughness was measured using a Wyko NT9300 light interference optical microscope.

Examinations and analyses of the corrosive properties of nickel and nickel-alumina coatings were made with the use of potentiostat ATLAS Sollich, AtlasCorr and AtlasLab computer programs. A three-electrode measurement system included a measurement vessel with a saturated calomel electrode (as a reference elec-

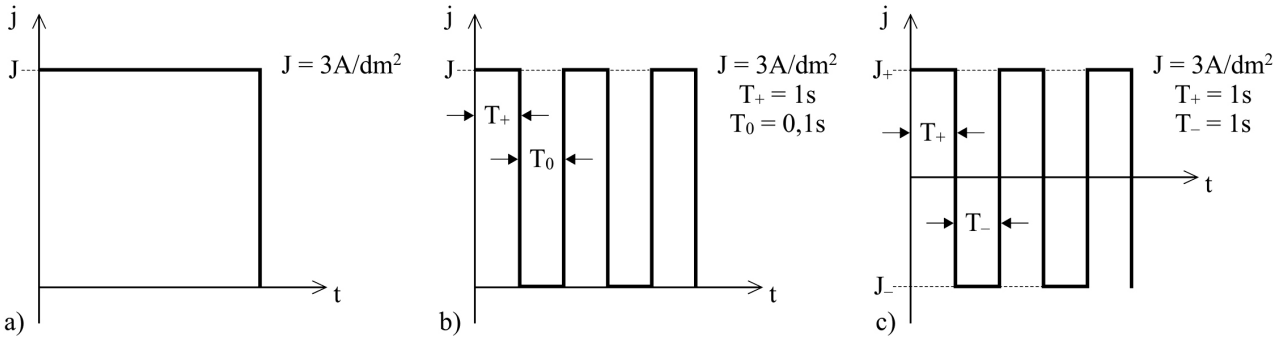

Figure 1: Scheme of impulse current and process parameters: a) DC, b) PC, c) PRC
Slika 1: Shema impulza toka in procesni parametri: a) DC, b) PC, c) PRC

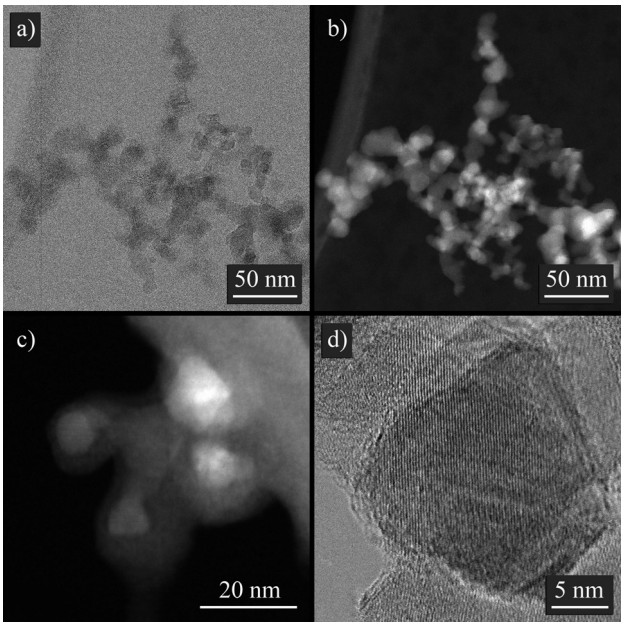

Figure 2: Microstructure of Al_2O_3 powder in: a) bright-field mode, b) Z-contrast mode, c) secondary-electron mode, d) bright-field mode
Slika 2: Mikrostruktura Al_2O_3 prahu: a) svetlo polje, b) Z-kontrast, c) sekundarni elektronski način, d) svetlo polje

trode), platinum mesh (as a counter electrode) and examined coatings (as a working electrode). The corrosion resistance was tested in the 0.5-M NaCl solution at 20 °C. The samples, before corrosive properties examination, were stabilized for 60 min in the target system as an open circuit. Research by electrochemical impedance spectroscopy was carried out in the corrosion potential surroundings in the frequency range 100 kHz to10 MHz of the10 mV amplitude.

The corrosion study was performed using the potentiodynamic method. For determining the polarization curves of the tested materials the measurements started from the potentials having values lower by 200 mV up to the values higher by 200 mV from the predetermined open-circuit potential with the potential scan rate equal to 0.2 mV/s and then up to 500 mV with a scan rate of 0.8 mV/s. The obtained curves were analyzed by the Tafel straight-lines method by keeping the conditions inherent in this method. The surface morphology of the examined materials after potentiodynamic tests was analyzed by scanning electron microscopy.

3 RESULTS AND DISCUSSION

Al_2O_3 powder was used as the dispersed phase in the Ni/Al_2O_3 composite coating formation process. The Al_2O_3 particles are presented in **Figures 2a** and **2b** in bright-field (BF) and Z-contrast modes, respectively. We can estimate from these images that their size is in the nanometric regime and it varies from 5 nm to 25 nm. Furthermore, the particles have the tendency to agglomerate, creating larger **Figures 2a** and 2**b** and smaller agglomerates, consisting of a few particles **(Figure 2c**). Images taken at higher magnifications (**Figure 2d)** showing crystallographic plates demonstrate that at least some of these nanoparticles are crystalline.

All coatings deposited from the basic Watts bath (Ni, Ni/Al_2O_3) have microcrystalline nickel structures (**Figures 3a** to **3f**). In the case of the use of the pulse reverse current the smallest grains are visible in the nickel and composite coatings. In turn the nickel and composite coatings produced in the electrolyte with grain growth inhibitor addition have a nanocrystalline structure

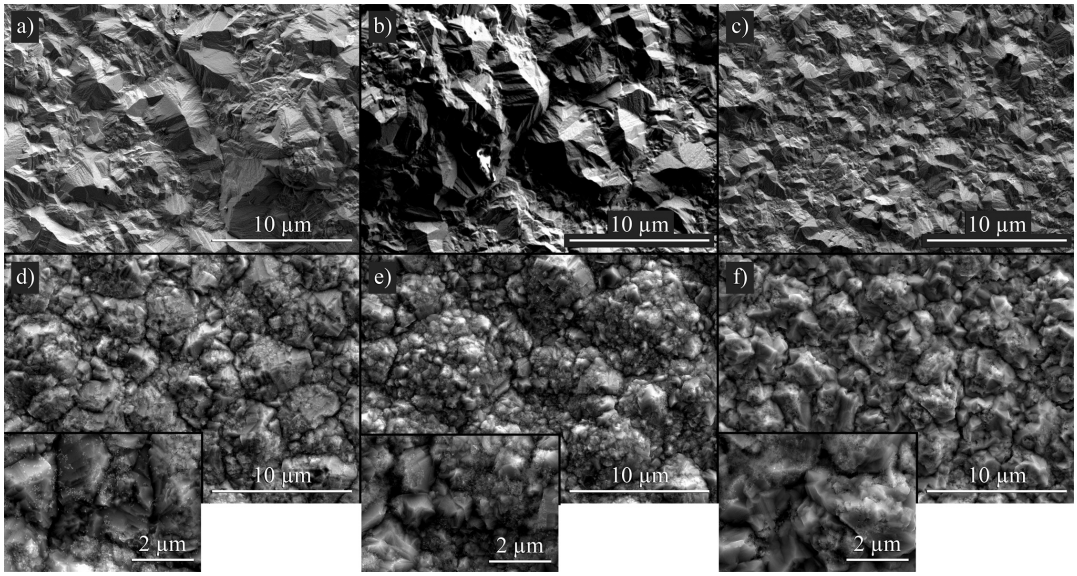

Figure 3: Morphology of microcrystalline coatings: a) nickel (DC), b) nickel (PC), c) nickel (PRC), d) Ni/Al_2O_3 (DC), e) Ni/Al_2O_3 (PC), f) Ni/Al_2O_3 (PRC)
Slika 3: Morfologija mikrokristaliničnih prevlek: a) nikelj (enosmerni tok), b) nikelj (pulzni tok), c) nikelj (impulznopovratni tok), d) Ni/Al_2O_3 (enosmerni tok), e) Ni/Al_2O_3 (pulzni tok), f) Ni/Al_2O_3 (impulznopovratni tok)

(**Figures 4a** to **4f**). The quality of the composite coatings with a nickel matrix and alumina dispersed phase depends on the formation of an appropriate structure with embedded alumina nanoparticles. The Al_2O_3 particles co-deposited in the nickel matrix cause a significant change in the morphology of its surface, as well the microcrystalline Ni matrix, as the nanocrystalline Ni matrix (**Figures 3a** to **3c**). The all $Ni_{\mu m}/Al_2O_3$ have large amounts of embedded disperse phase on its surface, which occurs often as agglomerates. In turn in the case of nanocrystalline composite coatings alumina is better fixed and distributed in the matrix. The nanocomposite coatings deposited with PRC were characterized by the largest surface roughness.

Due to this, one of the coatings was designated to TEM studies. The microstructure of the Ni_{nm}/Al_2O_3 coating obtained in the modified bath with PC was examined by STEM technique (**Figure 5**). The Al_2O_3 particles embedded in the matrix can easily be recognised as they stick out of the surface in **Figure 5a**) taken in SE-mode. Their existence was confirmed by X-ray EDS analysis (**Figure 5d**). In BF-mode (**Figure 5b**) as well as in

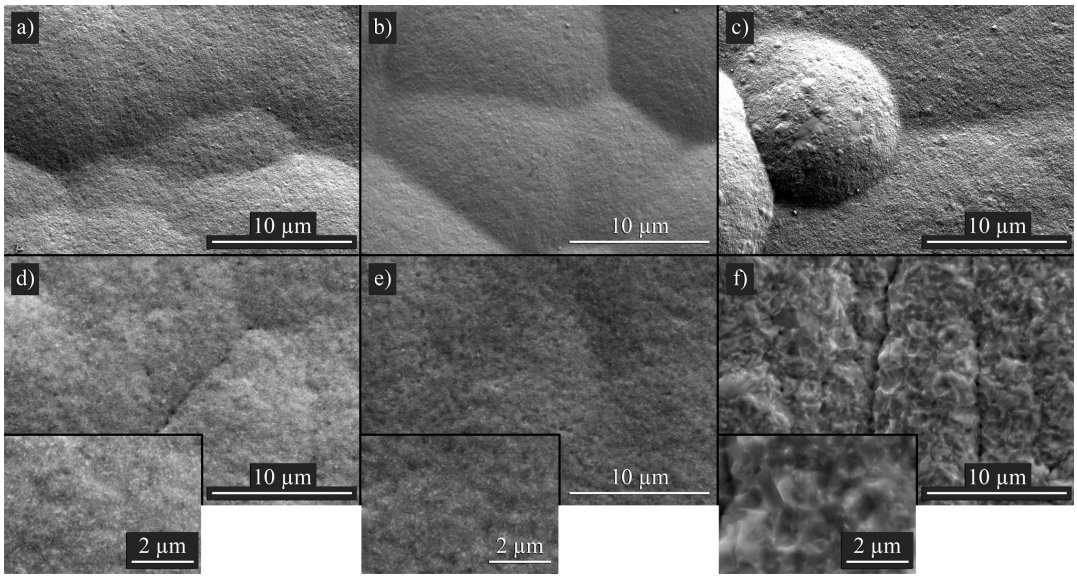

Figure 4: Morphology of nanocrystalline coatings: a) nickel (DC), b) nickel (PC), c) nickel (PRC), d) Ni/Al_2O_3 (DC), e) Ni/Al_2O_3 (PC), f) Ni/Al_2O_3 (PRC)

Slika 4: Morfologija nanokristaliničnih prevlek: a) nikelj (enosmerni tok), b) nikelj (pulzni tok), c) nikelj (impulznopovratni tok), d) Ni/Al_2O_3 (enosmerni tok), e) Ni/Al_2O_3 (pulzni tok), f) Ni/Al_2O_3 (impulznopovratni tok)

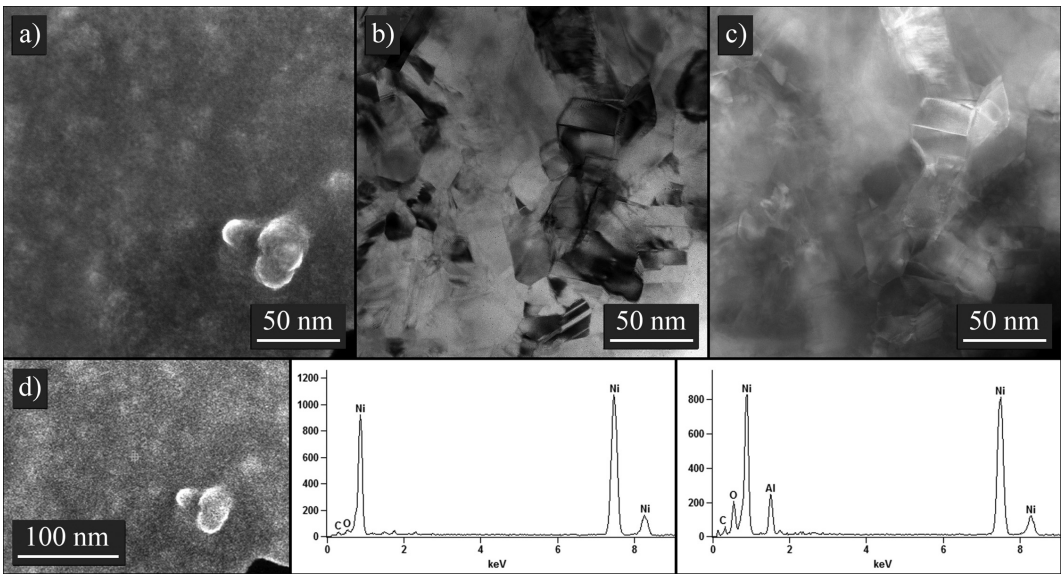

Figure 5: Microstructure and EDS result of Ni/Al_2O_3 coating obtained in the modified bath with PC: a) SE-mode, b) BF-mode, c) Z-contrast mode, d) EDS results

Slika 5: Mikrostruktura in EDS-analiza Ni/Al_2O_3 prevleke, pridobljene v spremenjeni kopeli z impulzivnim tokom (PC): a) SE-način, b) BF-način, c) Z-kontrastni način, d) rezultati EDS-analize

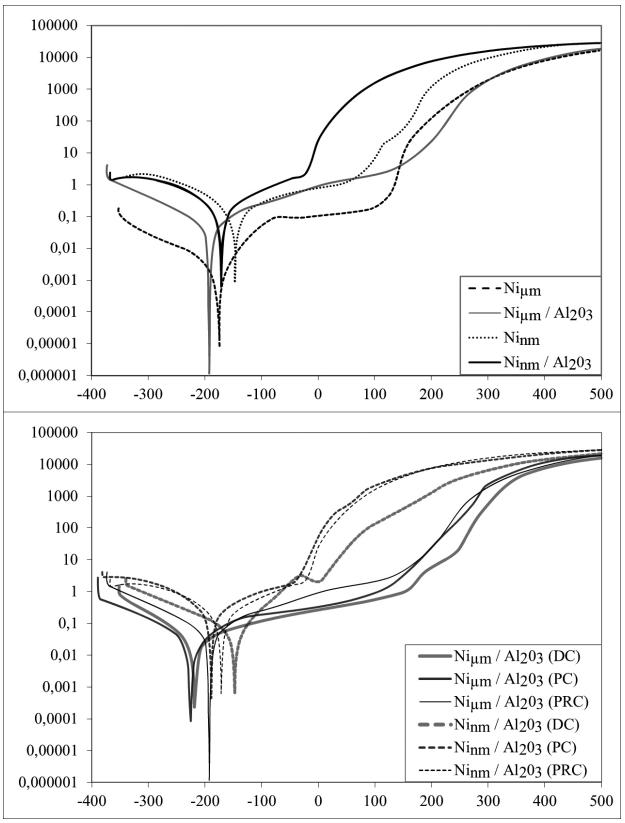

Figure 6: X-ray diffractogram of the nickel and Ni/Al_2O_3 composite coatings produced with DC in a Watts bath and a Watts bath with saccharine additives

Slika 6: XRD-analiza niklja in Al_2O_3 prevlek kompozitov, narejenih z enosmernim tokom in z Watts-ovo kopeljo z dodatki saharina

Z-contrast mode (**Figure 5c**) it is difficult to distinguish them from the matrix. In the matrix grains with an average 30 nm in diameter are present. In most of the grains dislocations can be found. Some of them are divided into sub-grains. Some contain annealing nano-twins.

X-ray analysis was performed to examine the effect of organic additive and the Al_2O_3 powder in the Watts bath on the structure of the nickel and composite coatings produced. The diffraction patterns of the coatings deposited with the DC current are shown in **Figure 6**. All the examined coatings are characterized by a crystalline structure. The profile diffraction lines indicate that the nickel coatings deposited in the base bath have the largest dimensions of the grains (79 nm and 88 nm, as estimated by the Scherrer equation). All the coatings produced with the addition of saccharine have nanocrystalline nickel structures. This is revealed by both the XRD patterns (**Figure 6**) and the images of the microstructure obtained by the SEM (**Figures 3** and **4**).

The diffraction line profiles (**Figure 6**) indicate that the composite coatings are characterized by a smaller dimension of crystallites: 26 nm and 18 nm and by 23nm and 15 nm, respectively, in comparison to micro- and nanocrystalline nickel.

The surface roughness of the examined coatings is shown in **Figures 7** and **8**. It can be seen from the 3D view of the surface profiles that the surface roughness is the highest in the case of the PRC coatings, followed by the DC and finally the PC coatings. The coatings

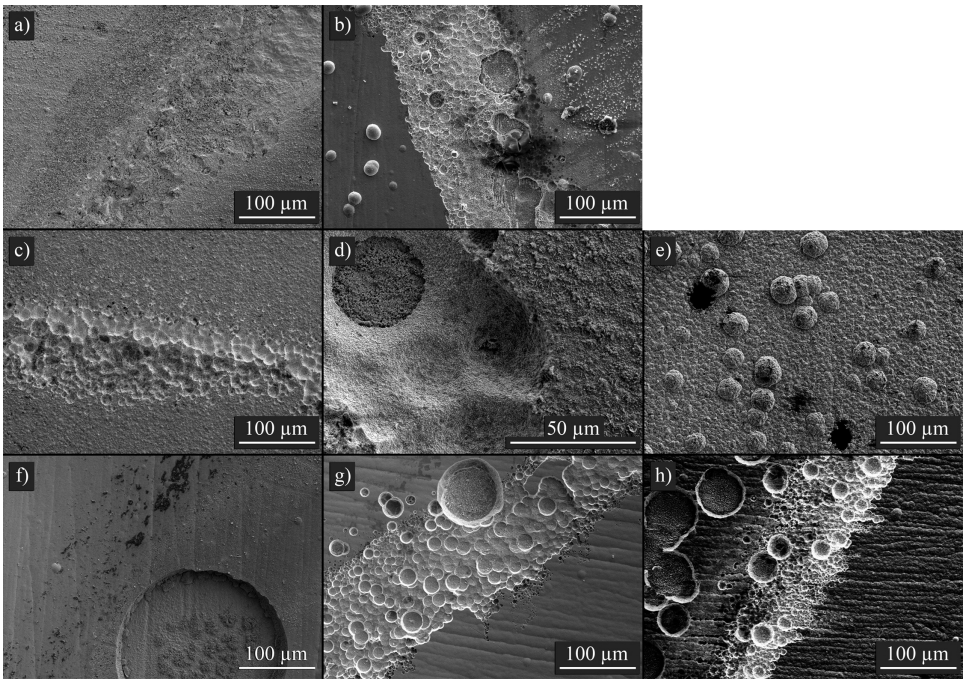

Figure 7: Surface roughness of microcrystalline coatings: a) nickel (DC), b) nickel (PC), c) nickel (PRC), d) Ni/Al_2O_3 (DC), e) Ni/Al_2O_3 (PC), f) Ni/Al_2O_3 (PRC)

Slika 7: Hrapavost površine mikrokristaliničnih prevlek: a) nikelj (enosmerni tok), b) nikelj (pulzni tok), c) nikelj (impulznopovratni tok), d) Ni/Al_2O_3 (enosmerni tok), e) Ni/Al_2O_3 (pulzni tok), f) Ni/Al_2O_3 (impulznopovratni tok)

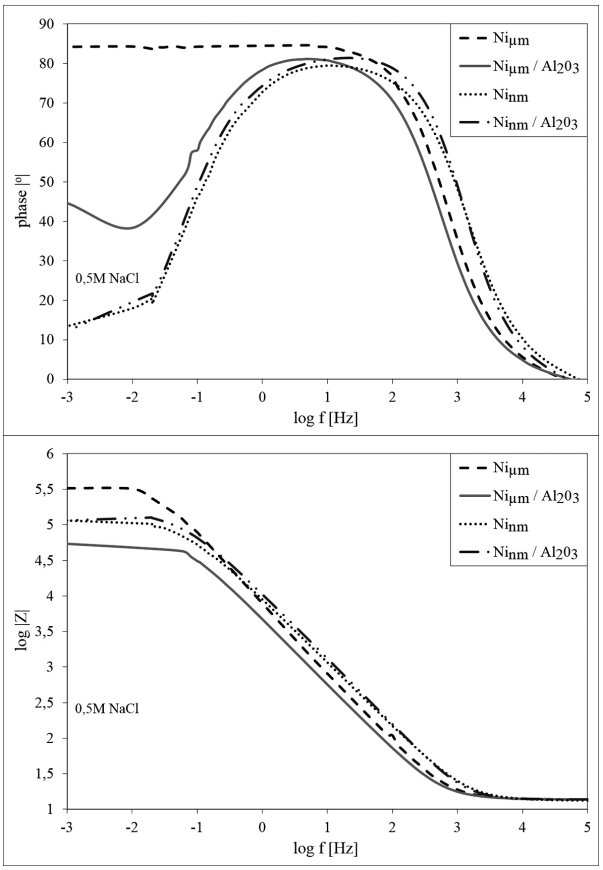

Figure 8: Surface roughness of nanocrystalline coatings: a) nickel (DC), b) nickel (PC), c) nickel (PRC), d) Ni/Al_2O_3 (DC), e) Ni/Al_2O_3 (PC), f) Ni/Al_2O_3 (PRC)

Slika 8: Hrapavost površine nanokristaliničnih prevlek: a) nikelj (enosmerni tok), b) nikelj (pulzni tok), c) nikelj (impulznopovratni tok), d) Ni/Al_2O_3 (enosmerni tok), e) Ni/Al_2O_3 (pulzni tok), f) Ni/Al_2O_3 (impulznopovratni tok)

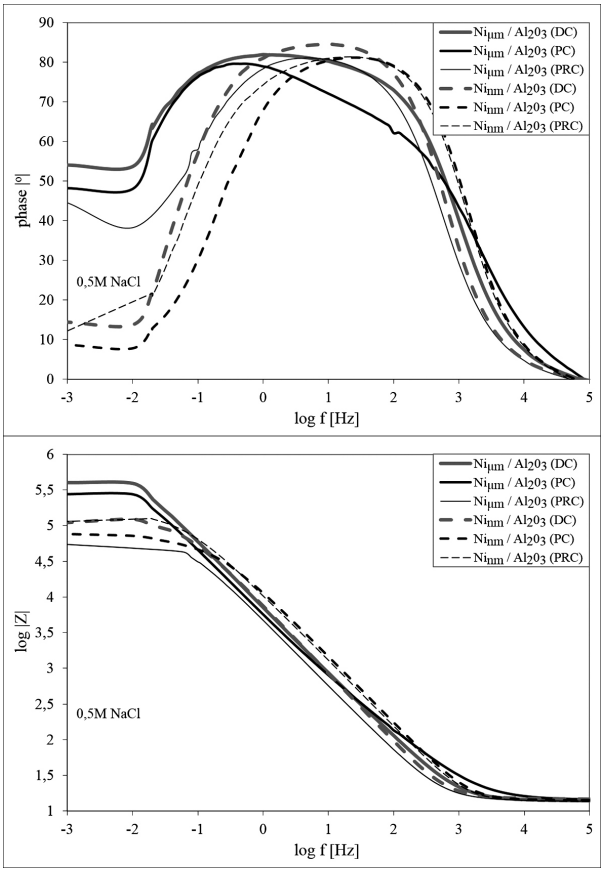

Figure 9: Polarization curves of Ni and Ni/Al_2O_3 coatings deposited with different current parameters

Slika 9: Polarizacijske krivulje niklja in Ni/Al_2O_3 prevlek pri različnih parametrih toka

deposited in the bath without organic additives are characterized by greater roughness (**Figure 7**). In the case of the DC and PRC microcrystalline coatings, the addition of Al_2O_3 makes the surface more irregular, which is visible both in 3D images and from the surface parameter characteristics (**Table 2**).

Table 2: Surface-roughness parameters

Tabela 2: Parametri površinske hrapavosti

		*R*a (nm)	*R*q (nm)	*R*t (nm)
$Ni_{\mu m}$	DC	162	207	1650
	PC	162	206	1520
	PRC	332	423	2930
$Ni_{\mu m}/Al_2O_3$	DC	286	388	3840
	PC	159	213	1870
	PRC	516	672	5120
Ni_{nm}	DC	100	132	1340
	PC	80	103	992
	PRC	141	178	1160
Ni_{nm}/Al_2O_3	DC	112	144	1050
	PC	55	70	525
	PRC	179	229	1970

Table 3: Characteristic parameters obtained as a result of potentiodynamic tests

Tabela 3: Karakteristike parametrov, pridobljene kot rezultat potenciodinamičnih testov

Material	Current	E_{corr} (mV)	i_{corr} (μA cm^{-2})
$Ni_{\mu m}$	PRC	-175	0.013
$Ni_{\mu m}/Al_2O_3$	DC	-218	0.048
	PC	-182	1.25
	PRC	-189	0.062
Ni_{nm}	PRC	-165	0.22
Ni_{nm}/Al_2O_3	DC	-147	0.056
	PC	-186	1.208
	PRC	-172	0.230

The results of the potentiodynamic method examinations are presented at **Figure 9**. The characteristic values are presented in **Table 3**. The potentiodynamic tests revealed that the nickel and composite coatings (with the exception of the composite coatings produced with PC) deposited in the basic Watts bath have good and similar corrosion properties, while the Ni_{nm} and Ni_{nm}/Al_2O_3 coatings obtained in the modified electrolyte (with a nano-nickel matrix) are characterized by increased corrosion potential and current density (**Table 3**).

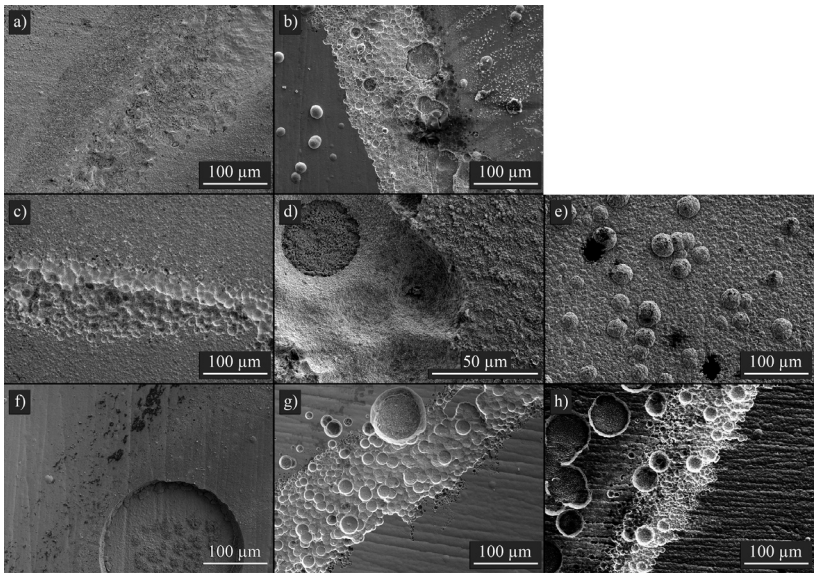

Figure 10: Morphology of the Ni and Ni/Al_2O_3 coatings after corrosion examinations: a) $Ni_{µm,}$ (PRC), b) Ni_{nm} (PRC), c) $Ni_{µm}/Al_2O_3$ (DC), d) $Ni_{µm}/Al_2O_3$ (PC), e) $Ni_{µm}/Al_2O_3$ (PRC), f) Ni_{nm}/Al_2O_3 (DC), g) Ni_{nm}/Al_2O_3 (PC), h) Ni_{nm}/Al_2O_3 (PRC)

Slika 10: Morfologija nikljevih in Ni/Al_2O_3 prevlek po korozijskih pregledih: a) $Ni_{µm,}$ (PRC), b) Ni_{nm} (PRC), c) $Ni_{µm}/Al_2O_3$ (DC), d) $Ni_{µm}/Al_2O_3$ (PC), e) $Ni_{µm}/Al_2O_3$ (PRC), f) Ni_{nm}/Al_2O_3 (DC), g) Ni_{nm}/Al_2O_3 (PC), h) Ni_{nm}/Al_2O_3 (PRC)

Table 4: Electric parameters of corrosion systems and schemes of the equivalent electric circuit for corroded coatings

Tabela 4: Električni parametri korozijskih sistemov in shem ekvivalentnega električnega tokokroga za korodirane prevleke

Material	Current	Electrical equivalent circuit	Electrochemical parameters						
			R_s (Ωcm^2)	R1 ($k\Omega cm^2$)	Y_01 ($\mu Fcm^{-2}s^{(n-1)}$)	n1	R2 ($k\Omega cm^2$)	Y_02 ($Fcm^{-2}s^{(n-1)}$)	n2
$Ni_{µm}$	PRC	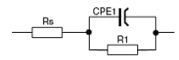	14.0	409	23.0	0.95	—	—	—
$Ni_{µm}/Al_2O_3$	DC	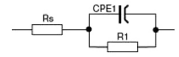	14.2	790	26.2	0.91	—	—	—
	PC	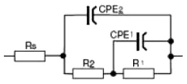	15.1	0.316	21.8	0.86	567	11.8	0.9
	PRC	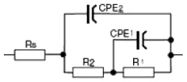	14.0	73.2	39.6	0.91	20.1	215.4	1.3
Ni_{nm}	PRC	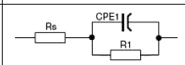	14.3	101	18.8	0.88	—	—	—
Ni_{nm}/Al_2O_3	DC	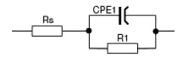	14.9	112	23.8	0.95	—	—	—
	PC	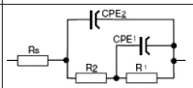	14.3	0.000000049	13.2	0.94	75.6	6.5	0.4
	PRC	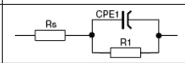	13.5	126	17.5	0.92	—	—	—

Together with an increase of the co-deposited alumina greater etching is visible (**Figure 10**) in comparison with the nickel coatings. Analyses of the electrodeposited nickel and composite coatings after exhibited in corrosion environments have demonstrated a pitting corrosion on the surfaces of the electrodeposited materials, except for the $Ni_{µm}$ and $Ni_{µm}/Al_2O_3$ deposited with PRC. The smallest corrosion degradation of the surface occurs in the case of the microcrystalline coatings (**Figure 10**).

The measured impedance spectra for the nickel and composite coatings deposited at different current parameters in the 0.5-M NaCl are shown as Bode diagrams in **Figures 11** and **12.** The fitting of the spectra obtained during the measurements based on the two equivalent electric circuits (**Table 4**) and enables an evaluation of

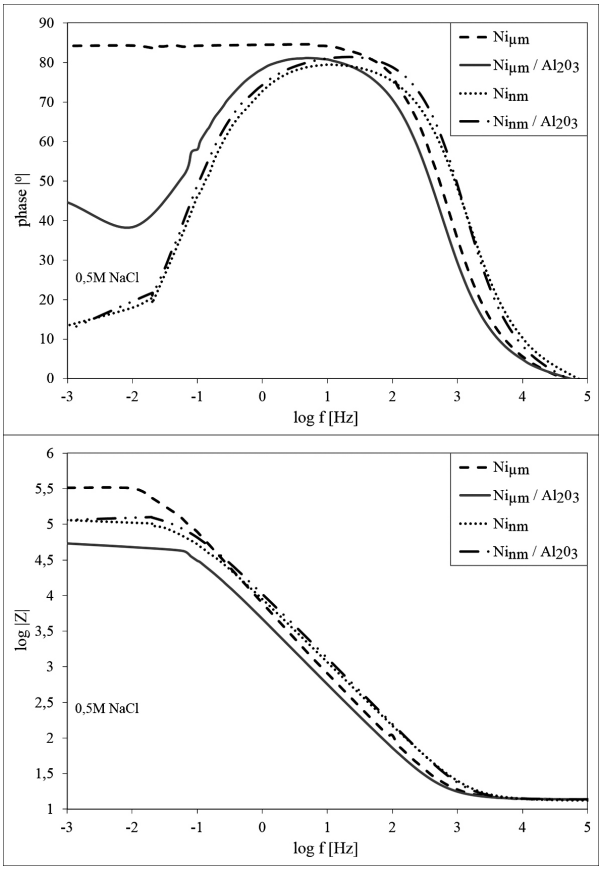

Figure 11: Bode spectra of the Ni and Ni/Al_2O_3 coatings deposited with PRC

Slika 11: Bode spektri Ni in Ni/Al_2O_3 prevlek pridobljenih z PRC

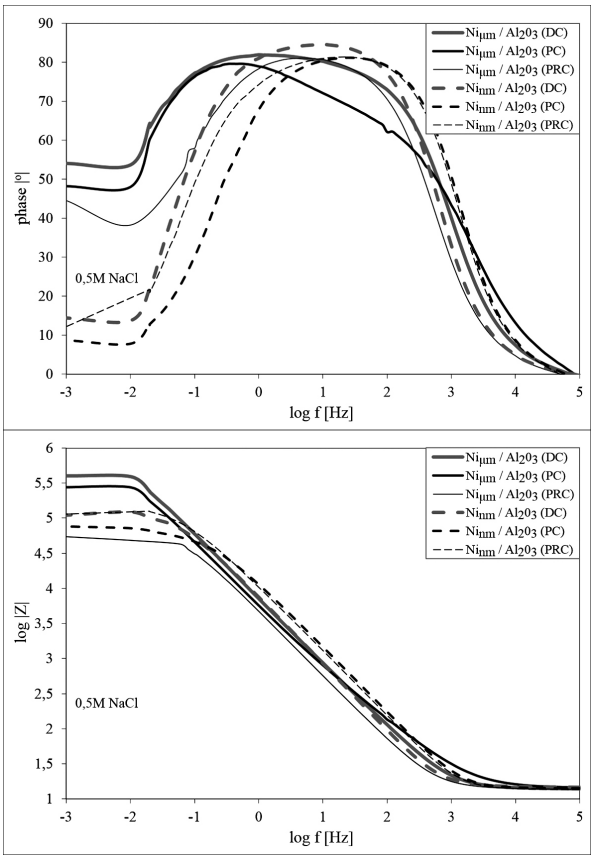

Figure 12: Bode spectra of the Ni/Al_2O_3 coatings deposited with DC, PC and PRC

Slika 12: Bode spektri Ni in Ni/Al_2O_3 prevlek pridobljenih z DC, PC in PRC

the corrosion properties. The equivalent electric circuits represent the process occurring in the corrosion system and allow us to define the parameters of these processes. In the electric models the element R_s reflects the resistance of the corrosion environment. The resistance of the electrolyte was comparable in all cases (**Table 4**). In contrast the element R1 characterizes the rate of corrosion process and it is connected with the resistance of the charge transfer across the interface. The capacity of these coatings reproduces the element $Y_0$1. Two additional elements in the second equivalent electric circuit: capacity of the surface area ($Y_0$2) and the resistance of the electrolyte in the area of the material (R2) are used in the cases of the coatings with higher roughness. The simple equivalent electric circuit (**Table 4**) was used in the case of the micro- and nanocrystalline nickel coatings deposited with PRC and the composite nickel coatings (both micro- and nanocrystalline nickel matrix) deposited with DC. It is related to the different structures of this coatings. For the $Ni_{\mu m}$ and $Ni_{\mu m}/Al_2O_3$ coatings deposited with PRC an increase in the phase-angle maximum is observed at low frequencies in contrast to the nickel and composite coatings with a nano-nickel matrix deposited with PRC (**Figure 11**). The $Ni_{\mu m}/Al_2O_3$ coating deposited with DC has the highest R1 value (790 kΩ cm^2, **Table 4**) and the widest range of maximum phase angle (**Figure 12**). In contrast the micro- and nanocrystalline composite coatings deposited with PC have the lowest R1, which indicates that there are surface-blocking processes.

Based on the analysis of the impedance phase-angle spectra, we found that microcrystalline coatings without Al_2O_3 phase are characterized by the highest corrosion resistance. Impedance phase-angle values have the maximum in a wide frequency range.

The incorporation of the ceramic phase in the microcrystalline nickel matrix results in the presence of boundaries between the embedded particles and the matrix, which is a place of corrosive attack. In particulalr, the Al_2O_3 phase in the case of coatings with microcrystalline matrix is incorporated in the form of several hundred nm agglomerates (**Figure 3d** to **3f**).

From the analysis of the impedance phase-angle spectra, we can also conclude that coatings with nanocrystalline nickel matrix have a decreased corrosion resistance. It is associated with a significantly larger number of grain boundaries, which also take the place of potential corrosive attack. Composite coatings with a nanocrystalline nickel matrix are characterized by

enhanced corrosion resistance compared to nanocrystalline nickel coating (wider range of maximum values of phase angle in the frequency range), which may either be due to the embedding of non-agglomerated, chemically resistant Al_2O_3 (**Figures 4d to 4f**) and the presence of the phase $AlNi_3$ (**Figure 6**).

In the case of coatings produced by the PC current method, a larger amount of built-in Al_2O_3 particles (**Figures 3e** and **4e**) is observed, resulting in a higher amount of interfacial boundary. These connections of the nickel matrix and the nanometric alumina particles are the target of corrosive attacks and therefore it results in the worst possible corrosion resistance.

4 CONCLUSIONS

Composite coatings are characterized by a smaller grain size compared to the pure nickel coatings obtained under the same conditions. Nickel and composite coatings deposited in a bath containing saccharine have a nanometric dimension of the crystallites, as compared to coatings produced in a basic Watts bath. In the case of the Ni_{nm}/Al_2O_3 composite coating, the presence of the $AlNi_3$ phase is also observed.

The surface roughness is the highest in the case of PRC coatings, followed by the DC and lastly the PC coatings. The coatings deposited in the bath with organic additives are characterized by a lower roughness.

Both the nickel and composite coatings deposited in the base Watts bath (microcrystalline coatings) have better corrosion properties in comparison with nanocrystalline coatings. The higher corrosion current and the greater destruction process (especially pitting corrosion) are visible in the case of nanocrystalline coatings.

The composite coatings deposited both in a base Watts bath and modified Watts bath with PC and PRC are characterized by different corrosion properties in comparison with the nickel and composite coatings deposited with DC. They are described by means of an advanced equivalent electric circuit (five-partial circuit).

The best corrosion properties, which are determined, e.g., by the phase-angle maximum and the corrosion destruction of surface, exhibit the $Ni_{\mu m}$ and $Ni_{\mu m}/Al_2O_3$ coatings deposited with PRC. The increase of the phase angle is observed at low frequencies in contrast to nickel and composite coatings with a nano-nickel matrix deposited with PRC.

5 REFERENCES

[1] R. K. Saha, T. I. Khan, Effect of applied current on the electrodeposited Ni-Al_2O_3 composite coatings, Surface and Coatings Technology, 205 (**2010**) 3, 890–895, doi:10.1016/j.surfcoat.2010.08.035

[2] B. Szczygiel, M. Kolodziej, Composite Ni/Al_2O_3 coatings and their corrosion resistance, Electrochimica Acta, 50 (**2005**), 4188–4195

[3] B. Kucharska, A. Brojanowska, K. Popławski, J. R. Sobiecki, Material Science, 21 (**2016**) 1, 31–35, doi:10.5755/j01.ms.22.1.7407

[4] M. Nowak, M. Opyrchal, S. Boczkal, J. Zelechowski, A. Najder, M. Karas, Effect of cathodic current density on microstructure and properties of nickel composite coatings, Archives of Metallurgy and Materials, 59 (**2014**) 1, 323–327, doi: 10.2478/amm-2014-0053

[5] B. Kucharska, K. Popławski, E. Jezierska, D. Oleszak, J. R. Sobiecki, Influence of stirring conditions on Ni/Al_2O_3 nanocomposite coatings, Surface Engineering 32 (**2016**) 7, 457–463, doi:10.1179/1743294414Y.0000000385

[6] H. Gul, F. Kilic, S. Aslan, A. Alp, H. Akbulut, Characteristics of electro-co-deposited Ni–Al_2O_3 nano-particle reinforced metal matrix composite (MMC) coatings, Wear 267 (**2009**) 5–8, 976–990, doi:10.1016/j.wear.2008.12.022

[7] B. Kucharska, J. R. Sobiecki, Microcrystalline and nanocrystalline nickel layers reinforced by Al_2O_3 particles, Composites Theory and Practice, 13 (**2013**) 4, 232–236

[8] L. Chen, L. Wang, Z. Zeng, J. Zhang, Effect of surfactant on the electrodeposition and wear resistance of Ni–Al_2O_3 composite coatings, Materials Science and Engineering, 434 (**2006**) 1–2, 319–325, doi:10.1016/j.msea.2006.06.098

[9] L. Chen, L. Wang, Z. Zeng, T. Xu, Influence of pulse frequency on the microstructure and wear resistance of electrodeposited Ni–Al_2O_3 composite coatings, Surface and Coatings Technology, 201 (**2006**) 3-4, 599–605, doi:10.1016/j.surfcoat.2005.12.008

[10] Y. S. Dong, P. H. Lin, H. X. Wang, Electroplating preparation of Ni–Al_2O_3 graded composite coatings using a rotating cathode, Surface and Coatings Technology, 200 (**2006**) 11, 3633–3636, doi:10.1016/j.surfcoat.2004.11.024

[11] M. Sabri, A. Sarabi, S. Kondelo, The effect of sodium dodecyl sulfate surfactant on the electrodeposition of Ni-alumina composite coatings, Materials Chemistry and Physics, 136 (**2012**) 2-3, 566–569, doi:10.1016/j.matchemphys.2012.07.027

[12] J. Chen, Characteristic of Ni-Al_2O_3 Nanocomposition Coatings, Procedia Engineering, 15 (**2011**), 4414–4418, doi:10.1016/j.proeng.2011.08.829

[13] Q. Feng, T. Li, H. Teng, X. Zhang, Y. Zhang, Ch. Liu, J. Jin, Investigation on the corrosion and oxidation resistance of Ni-Al_2O_3 nano-composite coatings prepared by sediment co-deposition, Metal Finishing, 107 (**2009**) 1, 34–41, doi:10.1016/S0026-0576(09)80007-X

[14] A. Góral, M. Nowak, K. Berent, B. Kania, Influence of current density on microstructure and properties of electrodeposited nickel-alumina composite coatings, Journal of Alloys and Compounds, 615 (**2014**), S406–S410, doi:10.1016/j.jallcom.2014.01.025

[15] C. Zanella, M. Lekka, P. Bonora, Influence of the particle size on the mechanical and electrochemical behaviour of micro- and nano-nickel matrix composite coatings, Journal of Applied Electrochemistry, 39 (**2009**), 31–38, doi: 10.1007/s10800-008-9635-y